Supersonic Shock Wave Turbulent Boundary-Layer Interactions

C. Herbert Law*
Aero Propulsion Laboratory, Wright-Patterson AFB, Ohio

Results are presented of an experimental investigation of shock wave turbulent boundary-layer interactions in supersonic flow. The experiments were conducted at a freestream Mach number of 2.96 and over a boundary-layer Reynolds number range of 10^5 to 10^6. Surface static pressure measurements, oil flow photographs, and interferograms were obtained to define the length of separation and the incipient separation angles for 1) two-dimensional compression corner and 2) planar shock wave interactions with a turbulent boundary layer. The tests were conducted in a high unit Reynolds number freestream on a long flat plate with a turbulent boundary-layer thickness in the interaction region of from 0.12 to 0.18 in. Direct comparisons were made between the compression corner and incident shock wave interactions to determine the effects of configuration on turbulent boundary-layer separation. For both configurations the length of the separated region was found to decrease and the incipient separation angle to increase with increasing Reynolds number. For constant Reynolds number, the overall pressure rise for incipient separation was approximately the same for the compression corner interaction and the incident shock wave interaction. Turbulent boundary-layer separation was found to be of the "free interaction" type whereby the separation angle and pressure distribution through separation were independent of Reynolds number, overall pressure rise, and configuration.

Nomenclature

C_{f0}	= skin friction coefficient at beginning of interaction
M, M_∞	= freestream Mach number
P	= pressure
P_0	= stagnation pressure
P_∞	= freestream pressure
$Re_{\delta 0}$	= Reynolds number based on freestream condition and boundary-layer thickness at beginning of interaction
S_{SG}	= span of shock generator
T_0	= stagnation temperature
T_w	= wall temperature
x	= axial distance from flat plate leading edge
x_c	= axial location of center of interaction
x_{LE}	= axial distance from flat plate/ramp hinge line to shock generator leading edge
x_s	= axial location of separation point
x^*	= axial offset distance
y_{LE}	= vertical distance between flat plate and shock generator leading edge
α_{IEFF}	= effective incipient separation corner angle
α_R	= compression ramp angle
α_{SG}	= shock generator angle
δ_0	= boundary-layer thickness at beginning of interaction

Introduction

THE interaction between a shock wave and a turbulent boundary layer is of practical importance because flow separation can significantly reduce both internal and external aerodyanmic performance and the resultant flow reattachment can severely magnify local aerodynamic heat transfer. There have been many investigations of turbulent boundary-layer separation produced by an impinging shock wave, a compression corner, and a forward facing step. However, the available experimental results are spread thinly over a wide range of Mach numbers and Reynolds numbers, and the effects of configuration on turbulent boundary-layer separation by indirect comparisons of isolated investigations are difficult to determine.

Received June 9, 1975; presented as Paper 75-832 at the AIAA 8th Fluid and Plasma Dynamics Conference, Hartford, Conn., June 16-18, 1975; revision received December 12, 1975.

Index categories: Boundary Layers and Convective Heat Transfer—Turbulent; Jets, Wakes, and Viscid-Inviscid Flow Interaction.

*Aerospace Engineer, Components Branch. Member AIAA.

Notable contributions have been made by Chapman, Kuehn, and Larson[1] and Holden,[2] to determine the effects of configurations on turbulent boundary-layer separation produced by a forward facing step, a compression corner, a curved compression ramp, and an incident shock wave in supersonic flow. By using similar model designs under the same wind tunnel conditions, direct comparisons were made to define the effects of configuration and variable Reynolds number and Mach number on boundary-layer separation. Holden performed similar investigations of the compression corner and incident shock wave interactions for hypersonic flow.

Recent surveys by Korkegi[3] and Green[4] indicate that while there is a general understanding of turbulent boundary-layer separation, specific agreement about the effects of Reynolds number and configuration on separation are lacking. Green concluded that much of the disagreement is the result of the boundary-layer interactions being strongly influenced by model design, but the detection methods or experimental procedures may themselves yield varying accuracies or degrees of sensitivity.

The compression corner interaction has been recently investigated by Settles, Bogdonoff, and Vas[5] and by Roshko and Thomke.[6] Roshko and Thomke simulated the compression corner with a large diameter cylinder/flare model and found that above a Reynolds number of 10^7, the incipient separation angle increased with increasing Reynolds number. Using a similar configuration and comparing with results obtained on a wind tunnel wall, Settles, Bogdonoff, and Vas found no dependence on Reynolds number over the same range. A similar investigation by Appels,[7] performed on a wind tunnel wall, found that while the incipient separation angle increased with increasing Reynolds number, the magnitude of the incipient separation angle was about half that observed by Settles, Bogdonoff, and Vas and by Roshko and Thomke.

Reda and Murphy[8] have investigated the effects of model design on the incident shock wave interaction, and found that three-dimensional effects can significantly influence a nominally two-dimensional interaction. In particular, the interaction between the incident shock wave and the wind tunnel wall boundary layer can produce significant effects if not properly isolated.

The present investigation was designed to provide a direct comparison between the interactions produced by the compression corner and incident shock wave configurations. Direct comparisons were made by producing the interactions on the same flat plate model in the same wind tunnel. A

Reynolds number range of 10^7 to 10^8 was investigated with a freestream Mach number of 2.96 and adiabatic wall conditions. The compression corner results have been previously reported in Ref. 9. A summary of these results and comparisons with the results obtained from the incident shock wave investigation are contained in this report. Surface pressure distributions, holographic interferograms, and oil flow photographs were obtained to define the undisturbed boundary-layer characteristics, the variations of separation length with compression corner angle and shock generator angle, and the incipient separation conditions. Three-dimensional effects were also investigated.

Experimental Procedure

The experimental procedures were discussed in detail in Ref. 9 and will only be summarized here. The experiments were conducted in the Aerospace Research Laboratories' 8-in. Mach 3 high Reynolds number wind tunnel. The Reynolds number was varied by changing the wind tunnel stagnation pressure. Four nominal Reynolds numbers were investigated: $Re_{\delta 0} = 1.5\times10^5$, 2.8×10^5, 60×10^5, and 9.0×10^5.

The model consisted of a 12-in.-long flat plate followed by a 2.5-in. compression ramp. The ramp angle could be varied continuously from 0 to 35 degrees by remote control during a run. The flat plate and compression ramp spanned the wind tunnel and were sealed at the sidewalls. The incident shock wave configuration consisted of a shock generator with a chord of 3.5 in. and the compression ramp placed in the 0° position. The shock generator could be remotely rotated from 0 to 15° producing an incident shock wave which intersected the flat plate/ramp hinge line. The span of the shock generator was 6 in. allowing 1 in. between the shock generator surface and the wind tunnel sidewall. This partial span configuration resulted in the least influence of sidewall interference (see the section on Three-Dimensional Effects).

The optical techniques, oil flow visualization, and pressure measurement techniques are described in Refs. 9 and 10.

Data were obtained for compression ramp angles of 14 to 26° in 1° increments, and for shock generator angles of 5.97 to 12.27° in approximately 0.5° increments. The shock generator angles were chosen to give the same overall pressure rises across the interaction as those produced by the compression ramp. The model configurations and corresponding shock generator/compression corner angles are shown in Figure 1.

Results and Discussion

Interferograms of the compression corner and incident shock wave interactions are shown in Figure 2. These interferograms show the basic structures of the interactions for an overall pressure rise of 4.85 p_∞ produced by a shock generator angle of 12.27° and a compression corner angle of 25°. These interferograms were obtained with $Re_{\delta 0} = 1.5\times10^{-5}$.

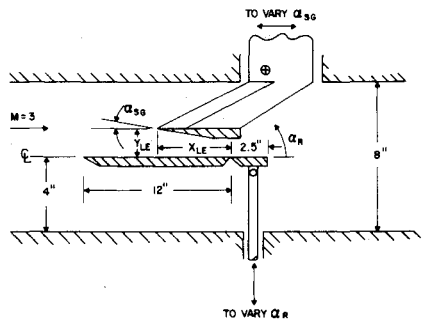

$\alpha_{R_{EFF}}$	α_{SG}	X_{LE}	Y_{LE}	$\alpha_{R_{EFF}}$	α_{SG}	X_{LE}	Y_{LE}
12.0	5.97	-3.41	1.50	19.0	9.39	-3.60	1.84
13.0	6.46	-3.44	1.55	20.0	9.87	-3.63	1.89
14.0	6.95	-3.47	1.60	21.0	10.35	-3.65	1.94
15.0	7.44	-3.50	1.64	22.0	10.83	-3.67	1.99
16.0	7.93	-3.52	1.69	23.0	11.31	-3.70	2.04
17.0	8.41	-3.55	1.74	24.0	11.79	-3.72	2.09
18.0	8.90	-3.58	1.79	25.0	12.27	-3.74	2.14

Fig. 1 Model and wind tunnel configuration.

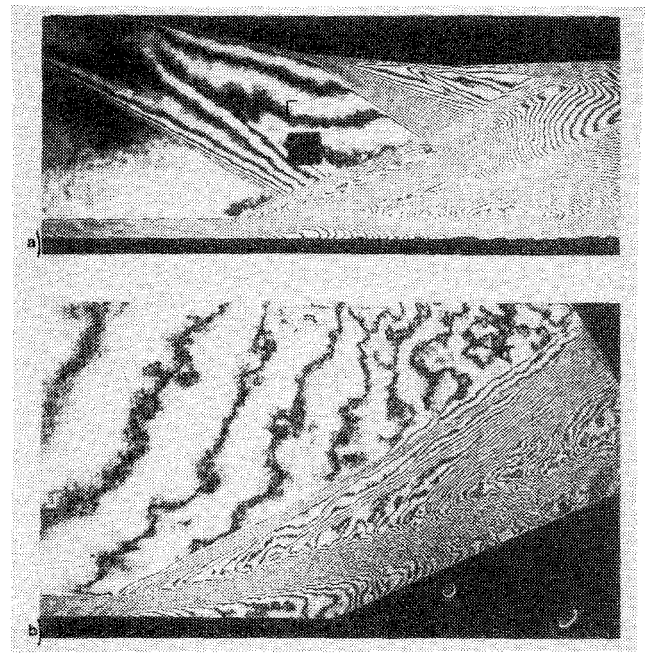

Fig. 2 Holographic interferograms of the compression corner and incident shock wave interactions with an overall pressure rise of 4.85 p_∞ for $Re\delta_0 = 1.5\times10^5$. a) Incident shock wave interactions $\alpha_{SG} = 12.27°$. b) Compression corner interaction $\alpha_R = 25°$.

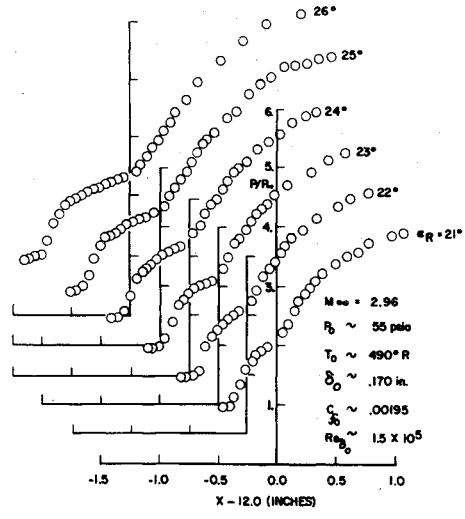

Fig. 3 Static pressure distributions for compression corner interaction.

For this investigation, the undisturbed boundary-layer thickness at the flat plate/ramp hinge line varied from 0.12 to 0.18 in. The high freestream Reynolds number and long flat plate were sufficient to produce natural boundary-layer transition well upstream of the interactions. The undisturbed boundary-layer velocity profiles (obtained from the interferograms) in the region of interaction agreed well with the $u/u_e = (y/\delta)^{1/7}$ power law. The large ratio of model span to boundary-layer thickness (~50) gave assurances that three-dimensional effects upstream of the interaction were minimal.

Examples of some of the static pressure distributions obtained from the incipient shock wave investigation are presented in Figure 3. Similar results obtained from the compression corner investigation are shown in Fig. 4. For all compression corner angles and shock generator angles investigated, the lengths of the compression ramp and shock generator were sufficient to achieve excellent agreement with the predicted overall pressure rise.

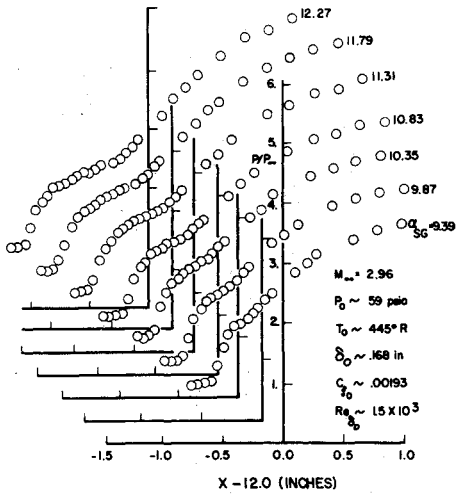

Fig. 4 Static pressure distributions for incident shock wave interactions.

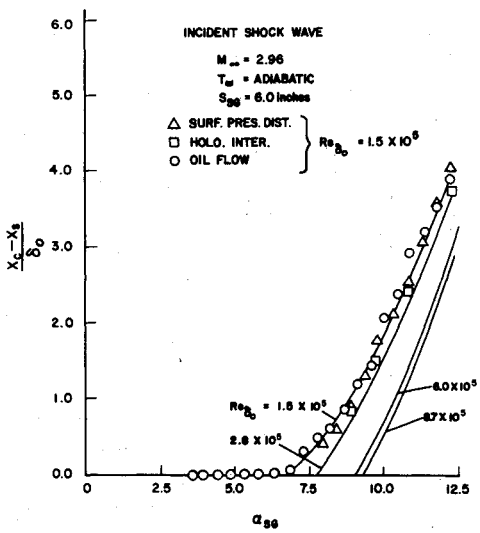

Fig. 5 Variation of the separation length with shock generator angle and Reynolds number.

Three techniques were used to determine the location of the separation point: 1) the axial location of the first inflection point in the static pressure distributions, 2) the location of oil accumulation, and 3) extrapolations of the separation shock wave to the flat plate surface. For large regions of separation, the three procedures gave reasonably good agreement for the location of the separation point, as demonstrated in Figure 5 for the incident shock wave investigation. For small regions of separation, the static pressure distribution and separation shock techniques were inadequate to provide separation information, and the oil flow technique gave questionable results. For both the compression corner and incident shock wave interactions, oil accumulation lines were present for overall pressure rise ratios below what would appear to be reasonable incipient values. The oil accumulation lines were thin (~0.020 in.) with positive (downstream) flow both upstream and downstream of the accumulation line. For the compression corner interaction, the oil accumulated on the surface along a line upstream of the corner, and yet, the surface oil flow in the immediate vicinity of the corner indicated positive, downstream flow. The oil flow technique, therefore, only gives the approximate location of the separation point as the axial location of some small value of skin friction. For large regions of separation this inaccuracy is not severe, but for small regions of separation (and below the incipient condition) the oil flow results were misleading.

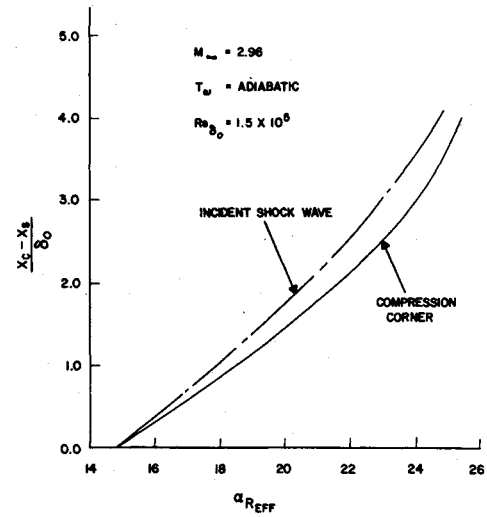

Fig. 6 Comparison between separation lengths obtained for the incident shock wave and compression corner interactions at the same freestream Reynolds number.

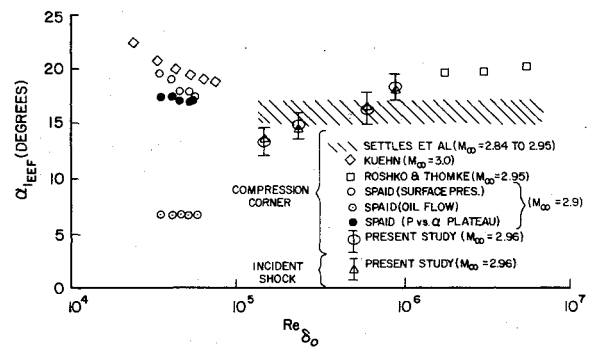

Fig. 7 Variation of the compression corner incipient separation angle with Reynolds number for a nominal Mach number of 3.

The length of separation results presented in Fig. 5 are compared with the results obtained from the compression corner investigation for the same Reynolds number in Fig. 6. In general, for the same overall pressure rise ratio, the incident shock wave configuration produced approximately a 15% larger length of separation than the compression corner configuration. The incipient separation angles (obtained by extrapolating to zero separation length) were approximately the same for both configurations. With the separation length nondimensionalized by the undisturbed boundary-layer thickness just upstream of separation, the separation length increased with decreasing Reynolds number for fixed overall pressure rise and the incipient separation angle increased with increasing Reynolds number. The incipient separation results from this investigation are shown in Fig. 7 and compared with results from other investigations.

Separation and Free Interaction

Chapman, Kuehn, and Larson[1] defined a "free interaction" as one which is free from direct influence of downstream geometry and free from the complicating influences of the mode of inducing separation. The occurrence of separation causes a change in the streamline geometry such that two separate shock-boundary-layer interactions are generated – the first where the flow separates and the second where it reattaches. For the separation interaction to be a "free interaction" it must be independent of downstream influence and the corresponding static pressure distribution be self-induced. According to the "dividing streamline" concept, the pressure rise in the reattachment region determines the mass of the recirculating flow and hence the length and

velocity of the dividing streamline. While the reattachment interaction is dependent on the configuration and overall pressure rise, the only influence these parameters have on the separation interaction is to determine its location.

In the present investigation the turbulent boundary-layer separation angle appeared to be relatively constant at approximately 11° for all compression corner angles and shock generator angles greater than incipient. Within the accuracy of the measurements (±1.50°) no consistent trend with Reynolds number was observed. These results were in good agreement with those presented by Erdos and Pallone[11] for the same Mach number and Reynolds number range.

The static pressure distribution through separation obtained from the present investigation is presented in Fig. 8. This distribution represents a sum of all the data obtained for shock generator angles and compression corner angles above incipient, and all Reynolds numbers investigated. The pressures have been nondimensionalized by the freestream static pressure. The axial distance has been offset so that the beginnings of pressure rise are coincident, and normalized by the undisturbed boundary-layer thickness. Over 400 data points were used to construct the pressure distribution which, within experimental scatter, reflects a "free interaction" similar to that observed by Zukoski[12] for flow ahead of a forward facing step. The pressure distribution was obtained by plotting only the pressure data in the separation and plateau regions. The pressure distributions downstream of the plateau, in the reattachment region, were not similar and therefore not of the "free interaction" type. Two examples of departure in the reattachment region are shown in Fig. 8 for a compression corner angle of 21° and a shock generator angle of 10.35°. In each case, the pressure distribution departs from the "free interaction" distribution in the reattachment region. The point of departure and the reattachment pressure gradient vary with overall pressure rise and configuration. As discussed earlier, for the same overall pressure rise, the incident shock wave produces a larger separation length than the compression corner.

A constant pressure plateau region was not observed in the present investigation because large lengths of separation were not achieved. The pressure distributions presented by Zukoski[12] indicated that separation lengths greater than about 7 boundary-layer thicknesses were required to achieve a constant pressure plateau region for turbulent flow. The pressure distributions obtained by Roshko and Thomke[6] from a compression corner investigation at Mach 4 were of the "free interaction" type similar to that presented in Fig. 8. Roshko and Thomke did investigate large lengths of separation and did observe constant pressure plateau regions for lengths of separation greater than 8 boundary-layer thicknesses.

Three-Dimensional Effects

The initial results of the present incident shock wave investigation with a full-span shock generator were in considerable conflict with the results obtained from the compression corner investigation. Oil flow visualization also indicated an extensive sidewall boundary-layer interaction and nontwo-dimensional flat plate boundary-layer interaction. Attempts to isolate the interior flat plate flow from the sidewall corner region with fences were unsuccessful. The only successful solution was to reduce the span of the shock generator until the influence of the sidewall interaction on the flat plate centerline flow was minimized.

The variations of separation length with shock generator span for several shock generator angles are shown in Fig. 9. These data were obtained at the lowest Reynolds number investigated. As the span of the shock generator was reduced, the strength of the sidewall interaction decreased. A shock generator span of 6 in. was sufficient to minimize the effects of sidewall interaction on the test region for shock generator angles less than 12.27°.

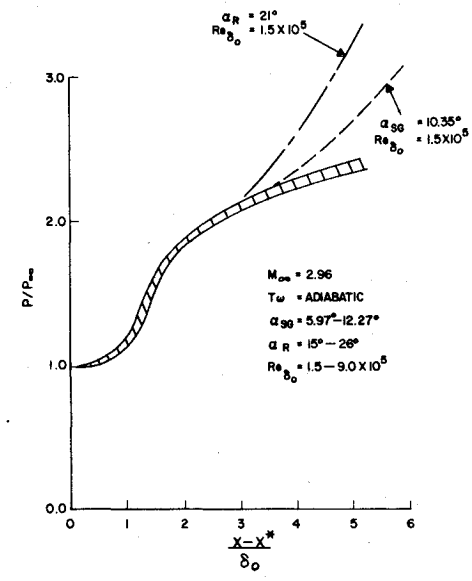

Fig. 8 Pressure distributions illustrating free interaction.

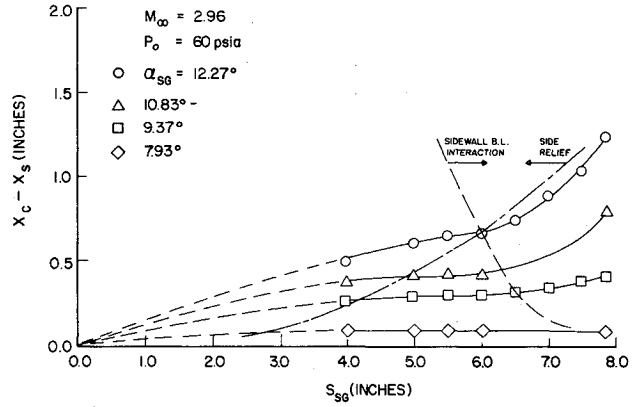

Fig. 9 Variation of the separation length with shock generator span.

Zukoski investigated the effects of span on the flow ahead of a forward facing step, and found a minimum span to avoid end relief. This minimum span was directly proportional to the step height and thus directly proportional to the length of separation. In the present incident shock wave investigation, a minimum span of the shock generator span was determined in order to avoid sidewall relief, and this minimum span was found to increase with increasing separation length, or shock generator angle. For a shock generator angle of 12.27° and an Re_{δ_0} of 1.5×10^5, the minimum span was found to be 6.0 in. Therefore, it was determined that the model design used in the present incident shock wave investigation could most nearly simulate a two-dimensional interaction on the flat plate centerline for shock generator angles up to 12.27° with a shock generator span of 6 in.

Conclusions

An investigation of shock wave-turbulent boundary-layer interactions at Mach 3 has been made. The effects of configuration have been determined by investigating 1) the compression corner, and 2) incident shock wave interactions over a range of Reynolds numbers (Re_{δ_0} from 10^5 to 10^6. The conslusions drawn from this investigation were as follows.

1) The separation length decreased and the incipient separation angle increased for increasing Reynolds number. 2) The overall pressure rise for incipient separation is independent of the configuration (compression corner or incident shock). 3) The three-dimensional effects of the interaction between the sidewall boundary-layer and the incident shock wave could be minimized by reducing the span of

the shock generator. 4) Turbulent boundary-layer separation was found to be of the "free interaction" type. The separation angle and the pressure distribution through separation were found to be virtually independent of Reynolds number, overall pressure rise, and configuration.

References

[1]Chapman, D.R., Kuehn, D.M., and Larson, H.K., "Investigation of Separated Flows in Supersonic and Subsonic Streams with Emphasis on the Effect of Transition," Ames Aeronautical Laboratory, Moffett Field, Calif., NASA Rept. 1356, 1957.

[2]Holden M.S., "Shock Wave-Turbulent Boundary Layer Interaction in Hypersonic Flow," AIAA Paper #72-74, San Diego, Calif., 1972.

[3]Korkegi, R.H., "Survey of Viscous Interaction Associated with High Mach Number Flight," *AIAA Journal*, Vol. 9, May 1971, pp. 771-784.

[4]Green, J.E., "Interaction between Shock Waves and Turbulent Boundary Layers," *Progress in Aerospace Sciences*, Vol. 11, Pergamon Press, pp. 235-340, 1970.

[5]Settles, G.S., Bogdonoff, S.M., and Vas, I.E., "Incipient Separation of a Supersonic Turbulent Boundary Layer at Moderate to High Reynolds Numbers," AIAA Paper #75-7, Pasadena, Calif., 1975.

[6]Roshko, A. and Thomke, G.J., "Flare-Induced Separation Lengths in Supersonic Turbulent Boundary Layers," AIAA Paper #75-6, Pasadena, Calif., 1975.

[7]Appels, C., "Incipient Separation of a Compressible Turbulent Boundary Layer," VKI Technical Note 99, von Karman Institute for Fluid Dynamics, Rhode Saint Genese, Belgium, Apr. 1974.

[8]Reda, D.C. and Murphy, J.D., "Shock Wave – Turbulent Boundary Layer Interactions in Rectangular Channels, Part II: The Influence of Sidewall Boundary Layers on Incipient Separation and Scale Washington, D.C. 1973.

[9]Law, C.H., "Supersonic, Turbulent Boundary Layer Separation," *AIAA Journal*, Vol. 12, June 1974, pp. 794-797.

[10]Havener, A.G. and Radley, R.J., "Supersonic Wind Tunnel Investigations Using Pulsed Laser Holography," ARL 73-0148, Aerospace Research Laboratories, Wright-Patterson AFB, Ohio, Oct. 1973.

[11]Erdos, J. and Pallone, A., "Shock-Boundary Layer Interaction and Flow Separation," *Proceedings on Heat Transfer and Fluid Mechanics*, pp. 239-254, 1962.

[12]Zukoski, E.E., "Turbulent Boundary-Layer Separation in Front of a Forward Facing Step," *AIAA Journal*, Vol. 5, Oct. 1967, pp. 1746-1753.

From the AIAA Progress in Astronautics and Aeronautics Series . . .

COMMUNICATIONS SATELLITE SYSTEMS—v. 32

Edited by P. L. Bargellini, Comsat Laboratories
A companion to Communications Satellite Technology, volume 33 in the series.

The twenty papers in this volume deal with international applications, advanced concepts, and special topics, covering the lessons and technical advancements resulting from the Intelsat II program of eight launches in the years 1966-1970. Includes Intelsat V system concepts and technology, with implications for multiple access, power generation and storage, and propellant utilization. It also includes proposals for U.S.-European cooperation in satellite applications programs of the Intelsat system.

Advanced concepts discussed include the coming generation of flexible communications satellites, with variations in switching, applications, and payloads; a dual-beam antenna for broadcast band service; high-powered, three-axis stabilized, position-keeping satellites; commercial communications with ships or aircraft via stationary satellites; multiple beam phased antennas; complex ground stations and relatively straightforward equipment on the satellite; and research in manned orbital laboratories.

Special topics include two-way telephonic communication via satellite, various education and information transfer systems, and a centralized radio-frequency data base for satellite communication system design.

480 pp., 6 x 9, illus. $14.00 Mem. $20.00 List

TO ORDER WRITE: Publications Dept., AIAA, 1290 Avenue of the Americas, New York, N. Y. 10019